CHARACTERIZATION OF A SILICON PYRAMIDAL NEURON

C. RASCHE, R.J. DOUGLAS, M. MAHOWALD
Institut für Neuroinformatik, ETH/UNI, Gloriastr. 32, Zürich 8006

The Silicon Neuron is an analog VLSI circuit that has the functional characteristics of real neurons. The circuit emulates many of the ion conductances that generate action potentials and control the dynamics of their discharge. The ion conductances are modeled according to the Hodgkin-Huxley principles. The voltage dependence of the ion channels is achieved by a transconductance amplifier that has a sigmoidal steady-state current voltage relation similar to that observed in biological active membrane channel conductances. The temporal dynamics of the conductances are emulated by a follower integrator. Intra-cellular calcium concentrations are also emulated, and used to obtain spike frequency adaptation in various forms, similar to real neurons. The parameters of the various circuits can be set so that the general Silicon Neuron circuit emulates a particular class of biological neurons. In this paper, we describe how the silicon neuron can be configured to emulate a neocortical pyramidal cell.

1 Introduction

In previous communications [1] we described the principles required to build Silicon Neurons (SN) using CMOS analog VLSI technology. In this publication we present an elaboration of that SN that simulates the electrophysiological characteristics of cortical pyramidal neurons.

The circuits of the silicon neuron approximate the performance of the Hodgkin-Huxley [2] formalism for active neuronal membrane conductances. Transconductance amplifiers form the foundation of the circuits used to emulate the voltage dependent conductances, while follower integrators provide the necessary dynamics. The interaction of separate circuits for activation and inactivation yields the approximately bell-shaped temporal forms seen in the case of the sodium spike conductance (for example). This interaction is multiplicative in conventional conductance simulations, but in the SNs the interaction is modelled by subtraction.

When appropriately configured, the SN exhibits electrophysiological behaviour comparable with real pyramidal cells. Changes of conductances and kinetics of some channel conductances lead to action potential generation characteristics, such as spike frequency adaptation, similar to that observed in the real counterparts. The distribution of interspike interval distributions is also similar to those measured from real pyramidal neurons *in vitro*.

The interest of SNs rests in their possible incorporation into large scale artificial neuronal networks. The simplified neurons that are used in most ar-

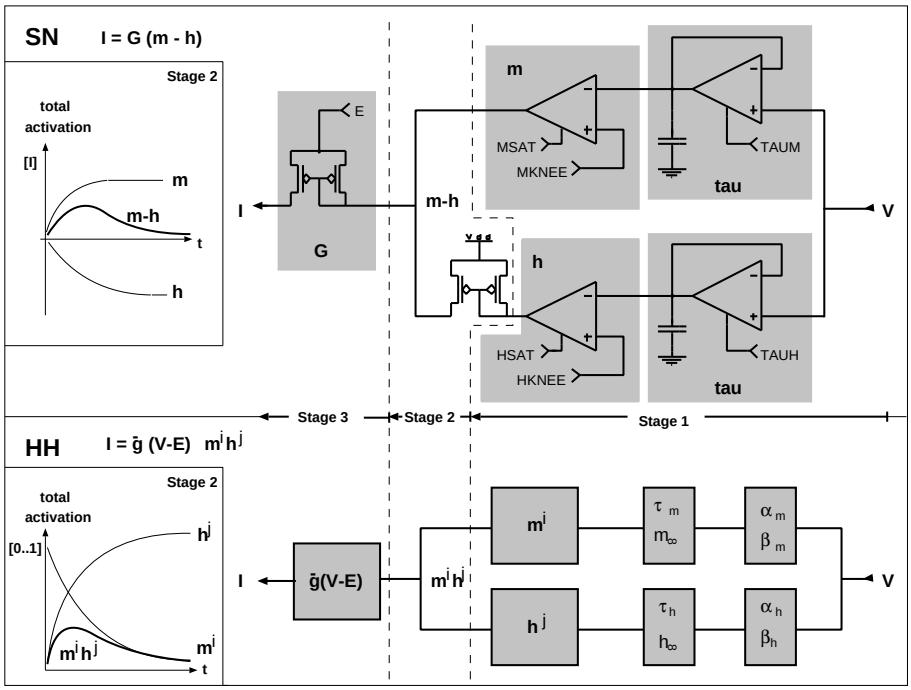

Figure 1: Analogy between the Silicon Neuron (**SN**) model and the Hodgkin-Huxley model (**HH**) of a channel conductance. **Stage 1, time and voltage dependences. HH**: The rate coefficients α_m and β_m (α_h, β_h respectively) are voltage dependent. These are used to determine τ_m and m_∞ (τ_h, h_∞). Box m^i represents the activation curve (h^j for inactivation) depending on time and voltage. i and j are exponents, usually between 1 and 4. m^i and h^j are normalized, ranging from 0 to 1. **SN**: *Time dependence* is implemented by a *follower integrator* (time element, grey box labeled tau), which low-pass filters the membrane voltage. The TAUM (TAUH) parameter determines the time constant of filtering. *Voltage dependence* is implemented by the *transconductance amplifiers* (activation and inactivation element, grey boxes labeled m and h). The KNEE parameter determines the threshold for activation of the conductance. SAT determines the strength of (in)activation. **Stage 2, combination of activation and inactivation. HH**: Activation and inactivation are *multiplied* to yield the bell-shaped temporal conductance (see graph total activation vs. time). **SN**: The two processes are currents *subtracted* by the current mirror right after the h-element (not in grey box). To obtain an optimal subtraction the parameter ratios MSAT/HSAT and MKNEE/HKNEE should be approximately equivalent. **Stage 3, calculation of output current. HH**: Total activation is multiplied by the term $\overline{g}(V - E)$ to yield the membrane current. **SN**: The 'total activation' signal controls a membrane conductance transistor which is part of a current mirror (conductance element, grey box labelled G). The membrane current flows from the common source voltage E, which represents the reversal potential of the ion, to the membrane capacitance (not shown).

tificial networks have an explicit output activation function. In real neurons the output activation function is not explicit. Instead, it depends on the states of the various somatic and dendritic conductances. Because the SNs emulate the electrophysiological behaviour of real neurons, they also inherit the properties that their output activation function need not be explicitly specified. This property is a useful step towards constructing artificial nervous systems that use more realistic principles of neural computation than do existing electronic neural networks. Moreover, the use of more realistic neurons improves the interface between engineering applications of neural networks, and the biological experiments that provide our understanding of such networks.

2 Methods

The present SN, which emulates the electrophysiology of the soma, consists of a somatic compartment and a simple dendritic load. The soma comprises five active conductances and one passive conductance: INA: sodium spike conductance, IKD: potassium spike conductance (delayed rectifier), IAHP: calcium-dependent potassium conductance, ICA: calcium conductance, ILEAK: passive leakage conductance. We use the term ion conductance rather than ion current, because the conductance reflects the average of many single ion currents that flow across the nerve cell's membrane. The aVLSI ion conductances are modelled according to the Hodgkin-Huxley-formalism[2]. The principles of this formalism are dissected into its elements, and each of them is electrically mimicked by a subcircuit. **Fig. 1** shows the analogy between between the Hodgkin-Huxley (HH) conductance model, and the aVLSI emulation. Computation of the channel conductance occurs in three stages, indicated from right to left. In real neurons the conductance (vs. time) is often bell-shaped. This form is achieved in the SN by subtracting a fast activating current from a slow inactivating current. **Fig. 2** shows the circuit of the basic actionpotential generation mechanism that includes the sodium (INA), the potassium (IKD) and the leakage conductance (ILEAK). **Fig. 3** shows the circuits that emulate the calcium conductance, the calcium concentration element, and the calcium dependent potassium (AHP) conductance. We assume that calcium enters the soma via a high threshold calcium conductance, so that calcium enters only during the ocurrence of a spike, and not simply during sub-threshold membrane depolarisation. The concentration element ([Ca]) tracks the concentration of intra-cellular calcium. The AHP conductance is activated by rising calcium concentration, and by lengthening the interspike interval, is responsible for spiking frequency adaptation.

The Silicon Neuron circuit is fabricated in a double-poly 2-μm CMOS

process on a MOSIS *tinychip*[1 3]. The subcircuits that emulate the various ion currents have a modular design, so that various conductance circuits can be incorporated or excluded from designs, as necessary. Furthermore, the currents that are included in any particular design can engaged or disengaged according to their parameter settings.

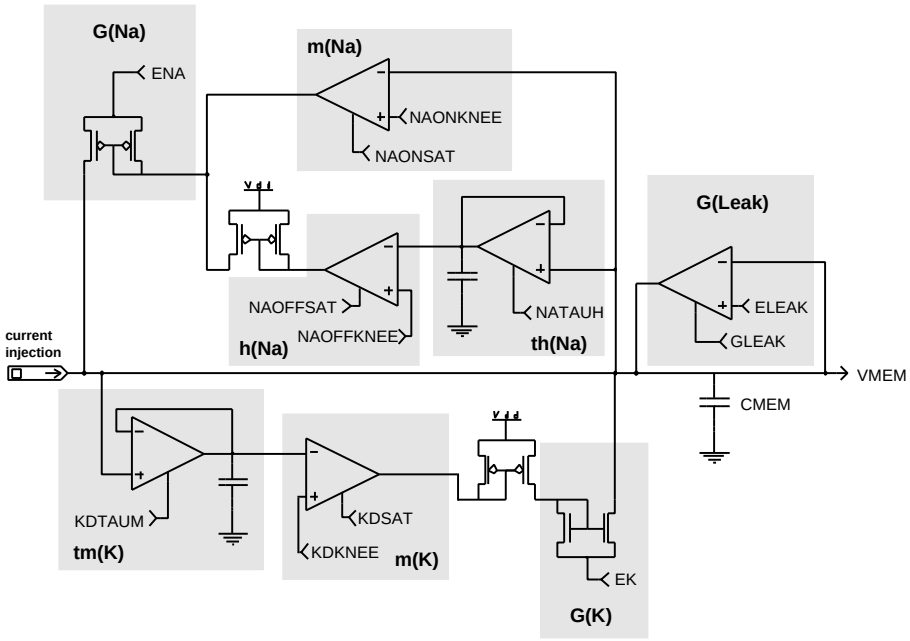

Figure 2: The analog circuitry of the basic spike mechanism. The horizontal wire carries the membrane potential (VMEM). The attached capacitor (CMEM) models the membrane capacitance. The boxed arrow on the left indicates a external current injection source. **Sodium (Na) spike conductance**. When external current injection drives membrane potential above NAONKNEE (representing firing threshold) a positive feedback loop (via m(Na) and G(Na)) drives the VMEM voltage to near ENA. Soon thereafter, inactivation (through th(Na) and h(Na)) occurs by subtracting current as explained in Fig. 1. **Potassium (K) spike conductance**. After onset of INA, the slower IKD turns on, and acts as a negative feedback loop, which pulls VMEM back down towards EK. **Leakage (Leak) conductance**. The follower-connected transconductance amplifier models the passive behaviour of the neuronal membrane. ELEAK is the resting potential, and GLEAK sets the leak conductance.

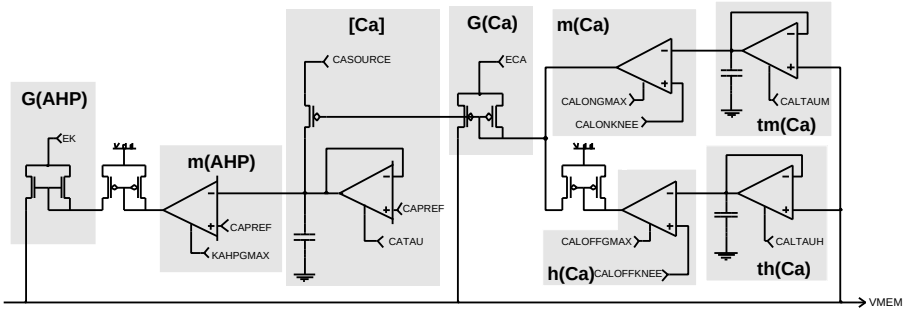

Figure 3: Calcium and calcium-dependent potassium (AHP) conductances and the calcium concentration element. The horizontal bottom line represents membrane voltage (VMEM). **Calcium (Ca) conductance**. Subtractive principle as described in Fig. 1. Every time a spike occurs calcium enters the cell through a high threshold calcium conductance. The calcium conductance also influences the spiking pattern. **Calcium concentration ([Ca])** module: A scaled copy of the calcium conductance drives the gate of the p-transistor and emulates calcium influx into the cell. This 'calcium' charge is stored on a capacitor. The follower provides calcium decay due to e.g. buffering. CATAU determines the time constant of calcium decay. CAPREF sets the calcium 'resting concentration'. **AHP conductance**: The wide-range-input transconductance amplifier (m(AHP)) senses calcium concentration voltage and determines the degree of activation of IAHP. The equilibrium potential in G(AHP) is tied to the same potassium equilibrium potential as in the basic spike mechanism. The AHP conductance constitutes a feedback loop (via [Ca]) that acts on a time scale of several tens of milliseconds. See also Fig 7.

3 Results

Fig. 4a shows examples of spike trains elicited by intrasomatic constant current injection. The arrow in the first plot shows where current injection starts. The lower trace in each plot represents the intra-cellular calcium concentration. A subthreshold current injection (0.37 nA) causes a simple, sub-threshold, charging response. A suprathreshold current injection (0.58 nA) causes an action potential discharge, and calcium enters the cell every time a spike occurs. The calcium decays exponentially by a constant rate. The range of current injection values (0.37 nA - 2.3 nA) shown is similar to range used in experiments on real neurons.

Spike frequency adaptation can already be seen in **Fig. 4**: the interspike intervals are short at first, and then increase in duration with successive intervals until a steady state discharge frequency is attained. **Fig. 4b** shows a family of output activation functions, or frequency-current curves, for this neuron. The rightmost curve shows the response for the first interspike interval. The remainder of the curves show responses for successive intervals (up to

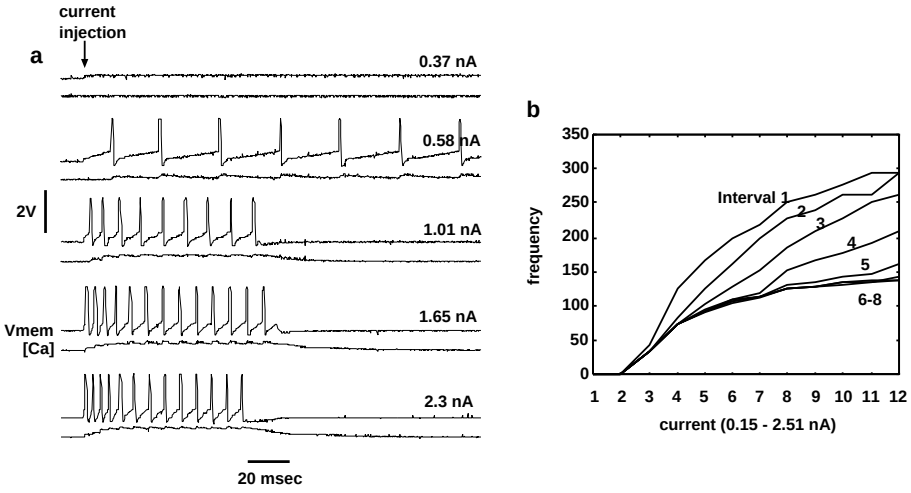

Figure 4: Response of the neuron to increasing current injections. **a.** Membrane voltage and calcium concentration in answer to 5 current stimuli. Noise in this recording arises mainly from quantization effects in the digitizing oscilloscope. **b.** Current-frequency curves in response to 12 current stimuli, showing saturation and spike frequency adaptation.

the eigth interval) as the neuron undergoes adaptation. For the first interval the current discharge relation has an initial steep slope and then saturates. The saturation is due to retarding effect on the occurence of the next spike, due to the post spike hyperpolarising conductance change (caused IKD). The slopes of the successive curves decrease as the adaptive conductance (IAHP) increases.

As in real cortical cells, the frequency of the first interval saturates at about 300 Hz for a current injection of about 2.5 nA. Later intervals (e.g. 5 and more) saturate at about 150 Hz. The current discharge relation for the first interval crosses the second at high current inputs, an effect also seen in biological neurons. This crossing is due to stronger hyperpolarization by the delayed rectifier following the broader first action potential, than later action potentials in a train.

Fig. 5 shows the interspike interval distribution for 1000 intervals as a probability density histogram. In a) noise-free constant current was injected and intervals we recorded after the neuron had adapted to its steady-state rate. In a purely deterministic simulation, a constant input stimulus would result in a constant interspike interval, and an interval distribution localised to a single bin. This is not the case in SN emulations, because like real neurons, the

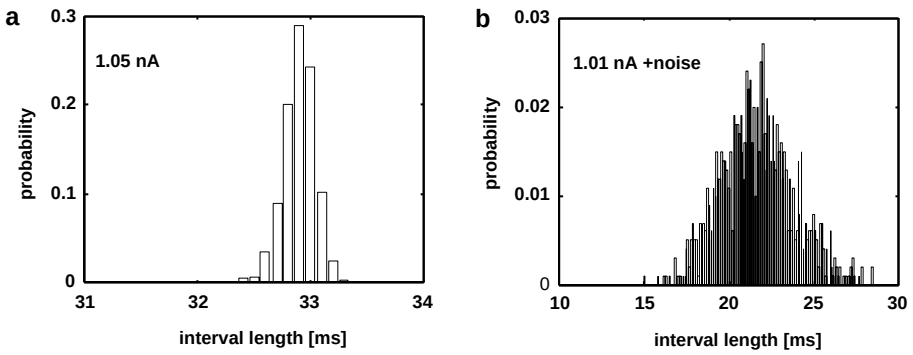

Figure 5: Interspike interval histogram of 1000 intervals with a bin size of 0.1 ms. **a.** Constant current injection. **b.** Noisy current injection.

overall performance of the SN is subject to noise in the physical components from which it is constructed. This noise leads naturally to variability in the duration of the interspike intervals. When Gaussian noise is added to the input current to emulate the form of typical dendro-somatic currents, the variability of the interspike intervals increases (b).

The detailed trajectories of the membrane potential during individual action potentials and the interspike intervals can be adjusted via parameter settings applied to the various ionic circuits. **Fig.6** shows the response of the neuron to the injection of pulses of 1nA amplitude and 5 ms duration, for values of the parameter KDTAUM. KDTAUM influences the dynamics of the potassium spike current. When the value of this parameter is small, IKD turns on late and so permits a broad spike width and consequently a large calcium influx. For larger values of the paramter, IDK turns on earlier, the spike becomes shorter, and the calcium influx is reduced. A very high value of KDTAUM results in premature activation of the potassium, so that the spike amplitude is attenuated.

A further example of parameter manipulation is shown in **Fig.7**. In this case the effect of manipulation of IAHP is illustrated. Two spike trains and their related calcium concentration are shown. Both these trains were evoked by the same current amplitude. In a) IAHP is turned on with the maximum conductance value. As anticipated, the IAHP activation slows down the firing rate and calcium concentration appears to saturate early, because the rate of calcium entry is restricted by adaptation of the spike rate. In b) the IAHP is switched off. No spike frequency adaptation occurs and calcium concentration saturates at a higher level, because of the elevated rate of calcium entry.

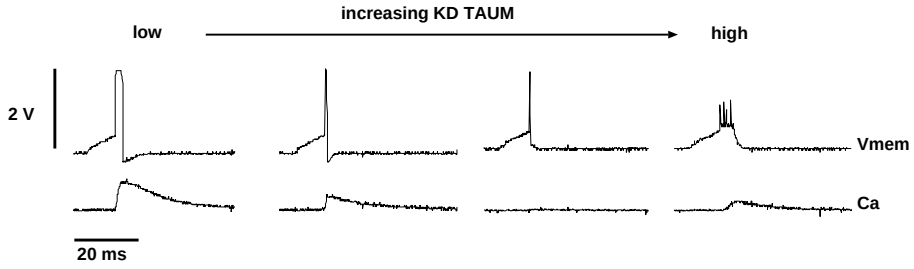

Figure 6: Action potential characteristics for KDTAUM. A low KDTAUM retards the activation of IKD resulting in a broad spike and large calcium influx. A large value causes premature activation of IKD, and so attenuates spike amplitude.

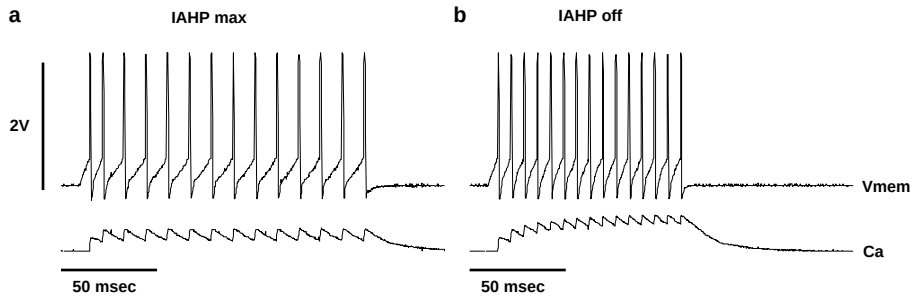

Figure 7: Effect of IAHP. Two spike trains elicited by the same stimulus current amplitude. **a.** When IAHP is turned conductance is large, spike frequency adaptation occurs, and calcium concentration saturates early. **b.** IAHP conductances is turned off, no spike frequency adaptation and calcium saturates late.

4 Discussion

The Silicon Neuron presented here offers a compact emulation of the Hodgkin-Huxley channel conductances in CMOS aVLSI. The parameters of the circuits can easily be set to emulate the electrophysiological performance of pyramidal neurons, and smooth neurons (data not shown) of cortex. So the SN could be used to emulate the anatomically defined networks of cortex. However, the SN has about 25 parameters and it is a time-consuming task to tune all of them to get the SN to spike. Therefore we require additional adaptive mechanisms to bring the SN into a stable spiking mode automatically. We are developing algorithms that bring the neuron into its spiking regime and also trim its spike frequency adaptation [4].

Additionally a model for intracellular calcium concentration was implemented. The dynamics of free, intracellular calcium are of particular interest, because the level of calcium controls activation of certain potassium conductances and is a reliable indicator of the cell's recent activity as well. The latter is being exploited by Shin who has implemented an algorithm for adaptive input gain control. Given these two algorithms the SN is independent of external adjustement and makes it suitable for large scale neuronal networks.

Acknowledgments

This work has been supported by the following institutions: UK Medical Research Council (MRC), Office of Naval Research (ONR), Gatsby Charitable Foundation and Centre Suisse d'Electronique et de Microtechnique (CSEM), Schwerpunktprogramm (SPP) Biotechnologie des Schweizerischen Nationalfonds.
We thank the following persons: Brian Baker for electronic support, and Dave Lawrence for programming device drivers.

References

1. M. Mahowald and R. Douglas. A silicon neuron. *Nature*, 354:515–518, 1991.
2. A.L. Hodgkin and A.F. Huxley. A quantitative description of membrane current and its application to conduction and excitation in nerve. *J. Physiol. (London)*, 117:500–544, 1952.
3. R. Douglas and M. Mahowald. A constructor set for silicon neurons. In Steven F. Zornetzer, Joel L. Davis, Clifford Lau, and Thomas McKenna, editors, *An Introduction to Neural and Electronic Networks*, chapter 14, pages 277–296. Academic Press, San Diego, CA, 2 edition, 1995.
4. J. Shin, C. Koch, and R. Douglas. Adaptive neural coding by monitoring the time varying somatic signal conditions. *to be submitted*, 1997.